



# Performance and Vibration of 30 cm Pyrolytic Ion Thruster Optics

Thomas Haag and George C. Soulas  
Glenn Research Center, Cleveland, Ohio

## The NASA STI Program Office . . . in Profile

Since its founding, NASA has been dedicated to the advancement of aeronautics and space science. The NASA Scientific and Technical Information (STI) Program Office plays a key part in helping NASA maintain this important role.

The NASA STI Program Office is operated by Langley Research Center, the Lead Center for NASA's scientific and technical information. The NASA STI Program Office provides access to the NASA STI Database, the largest collection of aeronautical and space science STI in the world. The Program Office is also NASA's institutional mechanism for disseminating the results of its research and development activities. These results are published by NASA in the NASA STI Report Series, which includes the following report types:

- **TECHNICAL PUBLICATION.** Reports of completed research or a major significant phase of research that present the results of NASA programs and include extensive data or theoretical analysis. Includes compilations of significant scientific and technical data and information deemed to be of continuing reference value. NASA's counterpart of peer-reviewed formal professional papers but has less stringent limitations on manuscript length and extent of graphic presentations.
- **TECHNICAL MEMORANDUM.** Scientific and technical findings that are preliminary or of specialized interest, e.g., quick release reports, working papers, and bibliographies that contain minimal annotation. Does not contain extensive analysis.
- **CONTRACTOR REPORT.** Scientific and technical findings by NASA-sponsored contractors and grantees.

- **CONFERENCE PUBLICATION.** Collected papers from scientific and technical conferences, symposia, seminars, or other meetings sponsored or cosponsored by NASA.
- **SPECIAL PUBLICATION.** Scientific, technical, or historical information from NASA programs, projects, and missions, often concerned with subjects having substantial public interest.
- **TECHNICAL TRANSLATION.** English-language translations of foreign scientific and technical material pertinent to NASA's mission.

Specialized services that complement the STI Program Office's diverse offerings include creating custom thesauri, building customized databases, organizing and publishing research results . . . even providing videos.

For more information about the NASA STI Program Office, see the following:

- Access the NASA STI Program Home Page at <http://www.sti.nasa.gov>
- E-mail your question via the Internet to [help@sti.nasa.gov](mailto:help@sti.nasa.gov)
- Fax your question to the NASA Access Help Desk at 301-621-0134
- Telephone the NASA Access Help Desk at 301-621-0390
- Write to:  
NASA Access Help Desk  
NASA Center for Aerospace Information  
7121 Standard Drive  
Hanover, MD 21076



# Performance and Vibration of 30 cm Pyrolytic Ion Thruster Optics

Thomas Haag and George C. Soulas  
Glenn Research Center, Cleveland, Ohio

Prepared for the  
39th Joint Propulsion Conference and Exhibit  
cosponsored by AIAA, ASME, SAE, and ASEE  
Huntsville, Alabama, July 20-23, 2003

National Aeronautics and  
Space Administration

Glenn Research Center

Available from

NASA Center for Aerospace Information  
7121 Standard Drive  
Hanover, MD 21076

National Technical Information Service  
5285 Port Royal Road  
Springfield, VA 22100

Available electronically at <http://gltrs.grc.nasa.gov>

# PERFORMANCE AND VIBRATION OF 30 CM PYROLYTIC ION THRUSTER OPTICS

Thomas Haag and George C. Soulas  
National Aeronautics and Space Administration  
Glenn Research Center  
Cleveland, Ohio 44135

Carbon has a sputter erosion rate about an order of magnitude less than that of molybdenum, over the voltages typically used in ion thruster applications. To explore its design potential, 30 cm pyrolytic carbon ion thruster optics have been fabricated geometrically similar to the molybdenum ion optics used on NSTAR. They were then installed on an NSTAR Engineering Model thruster, and experimentally evaluated over much of the original operating envelope. Ion beam currents ranged from 0.51 to 1.76 A, at total voltages up to 1280 V. The perveance, electron back-streaming limit, and screen-grid transparency were plotted for these operating points, and compared with previous data obtained with molybdenum. While thruster performance with pyrolytic carbon was quite similar to that with molybdenum, behavior variations can reasonably be explained by slight geometric differences. Following all performance measurements, the pyrolytic carbon ion optics assembly was subjected to an abbreviated vibration test. The thruster endured  $9.2 \text{ g}_{\text{rms}}$  of random vibration along the thrust axis, similar to DS-1 acceptance levels. Despite significant grid clashing, there was no observable damage to the ion optics assembly.

## INTRODUCTION

The low sputter erosion rate of carbon based ion optics has resulted in much interest from numerous organizations, including NASA, USAF, JPL, commercial companies, and foreign space agencies. Many financial efforts have been directed towards fabrication of carbon-carbon composite ion thruster optics since the early 1990's.<sup>1,5</sup> The successful integration of carbon materials into thruster optics is expected to increase propulsion system life by an order of magnitude.<sup>6</sup> Fabrication results thus far have been somewhat disappointing. While there are no obvious fundamental barriers to this goal, there are numerous limitations with existing fabrication techniques that have made fabrication of carbon NSTAR-class optics impractical. Small aperture size, high open area fraction, and thin screen grid thickness each represent compounding challenges to carbon material fabricators.

In order to exploit the structural strength of carbon fiber, continuous lengths of unbroken fiber tows must span length scales comparable to the ion beam diameter. With the NSTAR ion optics geometry, this amounts to weaving the fibers between adjacent screen apertures over a distance of about 30 cm.<sup>7</sup> Manual weaving of carbon fiber tows around thousands of aperture holes was found to be exceedingly tedious, and lacked the precise geometric definition required for effective aperture function. The inability to thoroughly densify the fiber matrix was also disappointing. Agencies in Japan claim to have been more successful with this type of design, but grid thickness and aperture size were significantly larger than those of NSTAR.<sup>5</sup>

While these results were fruitful, routine production was not implemented due to exceptionally high costs.

An alternate means of fabricating carbon-based ion thruster optics is through the use of pyrolytic carbon. This material is relatively isotropic in the planeular direction, with no directional fibers as in carbon composites. Pyrolytic carbon simplifies the fabrication process because there is no critical orientation in which aperture holes must be aligned with directional properties of material. While pyrolytic carbon does have a unique molecular orientation in the direction incident to the planeular surface, this orientation is easily accommodated with flat ion grid geometries. Pyrolytic carbon has been used routinely for many years on ground based ion accelerator equipment. Flight applications, however, will be much more demanding. The elastic modulus of pyrolytic carbon is an order of magnitude lower than that of carbon-carbon composites. Characteristic structural vibration will thus be at lower frequencies, and larger displacements. Also, ion thruster geometry is more thin and delicate than that used for typical industrial applications. Minimum web thickness between adjacent aperture holes are as thin as 0.3 mm, and require careful drilling.

NASA GRC initially procured an 8 cm diameter set of pyrolytic carbon grids with aperture geometry similar to that of NSTAR. Tests performed on those grids were encouraging, and showed comparable behavior to molybdenum grids of similar design.<sup>8</sup> The grids were flat however, and the low elastic modulus of pyrolytic carbon permitted undesirable variation of grid gap. Electrostatic attraction between the screen and accelerator grid could momentarily reduce the gap by

as much as 30% with application of high voltage, and could seriously complicate thruster operation. The problem will worsen drastically with larger diameter designs, as long as flat grid geometry is used. By dishing, or introducing spherical curvature to the grids, enormous increase in stiffness is possible. The NSTAR 30 cm design was recently fabricated in pyrolytic carbon so that its performance might be compared directly with the molybdenum design flown in DS-1. The following paper reports on results of those performance tests, as well as a random vibration test intended to verify the structural integrity of pyrolytic carbon under simulated launch conditions.

## TEST APPARATUS

### Pyrolytic Carbon Optics

Pyrolytic carbon ion optics were fabricated with a 28.5 cm beam extraction diameter. Both screen and accelerator grids had spherical curvature. Circular aperture holes were mechanically drilled in a hexagonal arrangement, producing ion optics geometrically similar to those of NSTAR. The screen apertures were measured with pin gages in several locations, and found to have hole diameters uniform to within 0.03 mm. From this, it was determined that the perforated open-area fraction was 64%. Due to this high open area, web thickness between adjacent holes was quite thin. In a few places, the webbing had broken through during fabrication, resulting in small voids. In the worst case, the triangle formed between three adjacent screen apertures had dropped out. There were four locations on the screen grid where such defects existed. In all cases, the broken webbing was within about 2 cm from the grid perimeter, where plasma density is expected to be low. Pin gage measurements of the accelerator aperture diameters indicated an open-area fraction of 24%. The screen and accelerator grids were attached to pyrolytic carbon stiffening rings with machine screws around the grid perimeter. The accelerator assembly was connected to a NSTAR mounting ring with 12 ceramic insulator posts. Flexure assemblies on each insulator permitted free radial movement between the accelerator and mounting ring. This was needed because the thermal expansion of the titanium mounting ring was much higher than the pyrolytic accelerator. There was concern that radial stress within the accelerator could lead to significant grid gap change or aperture misalignment. The flexures were rigid in the axial and azimuthal directions, securing the accelerator alignment even during launch vibration. Grid gap measurements revealed a curvature distortion in the pyrolytic carbon grids that affected a small sector of the optics assembly. This occurred at about half radius from the center, and was limited to a region several

centimeters in diameter. In this region, grid gap was as much as 45% less than at the perimeter of the optics assembly. Since grid gap was only controlled around the perimeter, the problem was reduced slightly by biasing the perimeter gap adjustment in that sector. Centerline grid gap was also slightly off, but by a much smaller degree.

### Discharge Chamber

For ion thruster performance measurements under vacuum, NSTAR Engineering Model thruster EMT3 was used. It consisted of a dc ring-cusp discharge chamber with a center mounted hollow cathode. The pyrolytic carbon ion optics assembly attached to the discharge chamber with six ceramic isolators. The discharge chamber and ion optics were enclosed inside a plasma screen and front mask in order to prevent electron back-streaming onto anode surfaces. An ion beam neutralization cathode was attached adjacent to the discharge chamber.

Due to its destructive nature, vibration tests were not performed with a functional ion thruster. The pyrolytic carbon ion thruster optics were reinstalled on NSTAR Engineering Model thruster EMT1c, which was structurally similar to the functional thruster, but with mass simulators in place of more delicate ancillary components. This thruster was mounted to a triple bi-pod strut assembly, representing gimbal attachment members for flight representative installations. The lower ends of the struts were bolted to the shaker table, as if the thruster was attached to a spacecraft rear bulkhead. Three control accelerometers were installed on the shaker table in close vicinity to the strut attachments.

## TEST FACILITIES

Tests were performed under vacuum in a 2.2 m dia. by 9 m long, horizontally oriented facility. Seven helium cryotubs provided a pumping speed of approximately 100,000 liters per second with xenon, and maintained pressures on the order of 0.5 mPa during thruster operation. The thruster was geometrically aligned to exhaust down the center axis of the facility, thus minimizing the flux of back-sputtered material. Electric power was provided to the thruster using rack-mounted laboratory power supplies. Thruster operating parameters were measured using isolated digital multimeters. Xenon propellant was supplied to the discharge cathode, main plenum, and neutralizer cathode. All flows were controlled and metered separately using commercially available flow controllers. A movable Faraday probe was used to collect plume data across the ion beam. The probe had a current collection area of 100 mm<sup>2</sup>, and was shunted

though a 1000 Ohm resistor. A two-dimensional positioning track allowed near-field horizontal probe sweeps to be taken within millimeters of the accelerator grid, or far-field sweeps 1.2 meters downstream of the exit plane. The probe location was computer controlled through two stepping motors on the two dimensional track. Probe signal data was digitized, and stored on magnetic disks.

Vibration tests were conducted in the Structural Dynamics Laboratory at the Glenn Research Center. This facility has a large electrodynamic shaker table, driven by a computer controlled power amplifier. It was capable of up to 155 kN of random vibration, with up to 38 mm pk-pk movement. Motion took place in the vertical direction only, parallel to the thrust axis of the ion optics. Three tri-axis accelerometers were attached to the EMT1c in order to assess cross-axis dynamic responses, and data signals were recorded electronically.

## TEST PROCEDURE

### Performance Measurements

Thruster performance was measured under vacuum inside the test facility described above. The ion beam neutralization cathode was ignited first, followed by the discharge chamber cathode. In these tests, neutralizer xenon flow was held constant at 3.60 sccm. Flow through the discharge cathode and main plenum were set according to the NSTAR throttle table. (See table 1) The thruster discharge was maintained for a minimum of one hour before beam extraction was attempted. This allowed time for thermal equilibrium to occur, improving repeatability of performance data. Thruster operating parameters were recorded manually, while plume probe measurements were recorded with a digital data acquisition system. The thruster was operated at beam voltages ranging from 650 to 1100 Vdc, and beam currents ranging from 0.51 to 1.76 A.

### Preparation for Vibration Test

There were some minor procedures performed on the ion optics assembly prior to vibrating. There were forty eight #2-56 stainless steel screws and nuts which attached the pyrolytic carbon electrodes to the stiffening rings. The threads of these screws were bonded with cyanoacrylic adhesive prior to the vibration test in order to prevent loosening. The adhesive was not compatible with high temperature vacuum, and could only be applied after the performance test was complete. A simple electrical circuit was installed across the screen and accelerator grid in order to monitor grid-to-grid contact during vibration. The accelerator grid was biased +9 volts

through a 1000 ohm resistor. A storage oscilloscope was used to monitor this voltage during vibration, where voltage drop would indicate instantaneous grid contact. This signal was also recorded in parallel with three tri-axial accelerometers mounted to the ion optics mounting ring. A debris collector was installed directly under the ion optics assembly in order to examine any particulate material generated during vibration. This was necessary because view of the screen grid was completely blocked by the accelerator grid. A small incandescent lamp was installed within the debris collector so that material thrown from the screen grid could be seen immediately.

### Vibration Test Procedure

Vibration tests were conducted after all performance data were obtained. Component tests were performed with the ion optics assembly removed from the thruster, and mounted to bookend-type supports. A miniature modal hammer was used to lightly impact directly at the center of the screen and accelerator grids. Vibration response of the individual grids were measured with a 0.14 gram accelerometer, and a non-contact fiber optic probe. Following the component tests, the ion optics assembly was installed on the EMT1c. All subsequent vibration tests took place in the vertical axis only, parallel to the thrust axis. A 1/8 g sine sweep was performed on the thruster in order to identify characteristic structural resonances. This sweep began at 5 Hz, and proceeded to 2 kHz at a rate of two octaves per minute. Random vibration testing was based on acceptance level specifications originally developed under the NSTAR program, which was also used as a basis for the DS-1 flight thruster test.<sup>9</sup> A listing of the frequency spectrum used in the random vibration test can be seen in table 2. Vibration levels were stepped up gradually, so that the maximum survivable level might be known. The vibration test was carried out in three phases, consisting of 20%, 50%, and finally 100% NSTAR acceptance levels. Each phase included about 15 seconds at the indicated level, followed by about one minute of quiet inspection. If no damage was detected during inspection, the next higher level began immediately. All vibration testing was carried out along the thrust axis, since this was judged to represent the worst case condition.

## RESULTS AND DISCUSSION

As mentioned in the Test Apparatus section, there were minor non-uniformities in the pyrolytic carbon grids that caused regional variation in grid gap. An initial performance map was generated with the screen to accelerator gap nominally set to 115% that of NSTAR. The nominal gap being the screen to accelerator

separation distance measured around the perimeter of the grids relative to NSTAR. Due to fabrication imperfections, this resulted in the centerline gap being 100%. Much of the following new results are presented at this gap setting, and showed somewhat lower performance compared to past NSTAR/DS-1 flight spare results.<sup>10,11</sup> It was decided to generate a second performance map at a screen to accelerator gap nominally set to 100% around the perimeter of the grids. Arguably, the hot centerline grid gap of NSTAR is less than that around the perimeter due to the higher thermal expansion rate of the molybdenum screen. Such cold/hot grid variation are less likely with pyrolytic carbon, but may be deliberately introduced for purposes of this comparison. With the perimeter set to 100%, the centerline grid gap was 87%.

Data obtained from operating at both grid spacings is listed in table 3. Also included is data referenced from the DS-1 flight spare thruster, which is of very similar construction except for the use of molybdenum ion optics.<sup>10,11</sup> At the lowest power level TH0, accelerator current for all three configurations is small. The molybdenum grids of DS-1 show slightly higher current, but the difference is comparable to scatter among all three. At the highest power level TH15, accelerator current for the two carbon grid configurations is about 4 mA higher than that referenced for DS-1. The vacuum facility pressure was comparable in each case, so it is unlikely that charge exchange is responsible for the difference. The difference in accelerator impingement represents about 0.23% of the beam current. While the four broken webs in the carbon screen grid are probably too small to account for this impingement current, distortions in the carbon grid gap may have contributed to the remainder.

### Radial Plume Profile

Profiles of the thruster plume were obtained by sweeping a faraday probe along the diameter of the thruster exit plane, several centimeters downstream of the accelerator grid. Examples can be seen in figure 1, where four superimposed profiles are shown at different beam currents. While beam current increases by a factor of 3.5 from TH0 to TH15, maximum beam current density increases by a factor of 2.5. This suggests that beam current density increases faster at the periphery region, resulting in a relatively flatter profile at higher power levels.

### Perveance Limit

Beam extraction capability for the molybdenum and carbon grids were compared at different beam currents. The accelerator impingement perveance limit was measured for both grid gap spacings using the NSTAR procedure. At each beam current, beam power supply

voltage was incrementally reduced until accelerator grid current increased rapidly. The point where accelerator grid current increased by more than  $-0.02$  mA/V was identified as the impingement-limited total voltage, and is plotted in figure 2 as a function of beam currents. Recent pyrolytic grid perveance at two spacings is compared with that measured from the DS-1 flight spare thruster. The impingement-limited total voltage for the 115% grid gap was typically 100 volts higher than that of the 100% grid gap. While the DS-1 flight spare thruster performed better than the pyrolytic carbon thruster, the narrow grid gap performance came fairly close. The accelerator holes in the pyrolytic carbon were slightly smaller than those in the molybdenum. Also, the carbon apertures were machine cut, with very cylindrical barrels. The molybdenum grids were chemically etched, and tapered on both sides. The tapered geometry may effectively delay accelerator aperture hole impingement, resulting in a wider range of beam extraction capability.

### Electron Backstreaming Limit

The electron backstreaming limit was determined by gradually reducing accelerator voltage magnitude at a fixed beam power supply voltage until the indicated beam current increased by 0.1 mA. The accelerator voltage at that point was identified as the electron backstreaming limit, and is listed in table 3 for each operating condition. A plot of electron backstreaming limit as a function of beam current is shown in figure 3. This includes data for both pyrolytic grid spacings, as well as data obtained from the DS-1 flight spare thruster. The plot shows that the pyrolytic accelerator grid has a significantly lower electron backstreaming limit than that of the molybdenum grids. Another predictable observation is that the 115% grid spacing is more effective than the 100% spacing at repelling electrons. At the lowest beam current, the molybdenum accelerator grid needed at least 18 additional volts negative potential in order to repel downstream electrons when compared to the carbon accelerator grid. At the highest beam current, the molybdenum accelerator grid needed a minimum of 46 additional volts as compared to the carbon grid. These results suggest that it would have been advantageous to increase the aperture diameter in the pyrolytic accelerator grid beyond what was used with the chemically etched molybdenum. This would likely increase perveance with little penalty in electron backstreaming, however the neutral xenon loss rate would increase. Significant improvement in life would be realized by using sputter resistant carbon, and by using mechanically machined cylindrical apertures. Chemically etched molybdenum usually leaves sharp cusps within each aperture, and these are subject to rapid wear, and premature enlargement to a larger inner diameter. Mechanical drilling of molybdenum is

probably not cost effective due to its hardness, and the tens of thousands of holes required in NSTAR type ion optics. Pyrolytic carbon is much softer to drill than molybdenum, and requires no cutting fluid.

### Screen Grid Transparency

Screen grid transparency was determined as the ratio of beam current over combined beam and screen current. A -20 volt bias was applied to the screen grid during operation in order to repel electrons, and ion collection current to the screen was thus measured. This process was performed at all operating points, with both 100% and 115% grid spacings. Results are listed in table 3, and show rough agreement with the nominal screen open-area-fraction of 67%. Figure 4 shows screen transparency to be relatively insensitive to beam current. Ion optics are penalized by space-charge effects as beam current increases, and a slight reduction in transparency can be seen at higher beam currents. On average, the carbon grids had about 0.1 (10%) lower transparency than molybdenum grids under similar operating conditions. This may be due to slightly lower open area fraction with the carbon grids, or it may be due to variation in experimental technique. The 100% grid gap resulted in slightly higher transparency than the 115% gap, which suggests that the position of the electrostatic sheath may be farther upstream with the narrower grid gap. Even though the molybdenum and carbon screens have the same thickness, the cusp in the molybdenum screen is likely very thin, reducing the effective thickness of the molybdenum screen grid. In this case, the chemical etched fabrication technique may work to an advantage.

### Diagnostic Vibration Tests

Individual component vibration tests were performed on the screen and accelerator grid in order to determine their natural frequency. A miniature modal hammer was used to lightly strike the center of each grid. The ringing response was observed using two methods. A 0.14 gram accelerometer was attached to the accelerator grid near the center, as shown in figure 5. When the modal hammer impacted the grid, it resonated with a frequency of 664 Hz. This frequency was confirmed by using a non-contact fiber optic displacement probe in place of the accelerometer. A similar test performed on the screen grid indicated a first mode natural frequency of 504 Hz. The lower frequency of the screen grid is likely due to its higher open area fraction.

Integrated assembly vibration tests were performed in order to verify structural integrity of the pyrolytic ion optics as part of a complete ion thruster. The pyrolytic carbon ion optics assembly was installed on NSTAR EMT1c. This thruster was non-functional, but was

structurally similar to the thruster flown on DS-1. Three bipod strut assemblies were attached at the gimbal interface pads of the thruster, as shown in figure 6. The lower end of the struts were bolted to the vibration table. Control accelerometers for the test were installed at the base of the struts, establishing the specified vibration intensity at the very base of the thruster. Additional accelerometers were installed on the ion optics mounting ring, which held the pyrolytic grids. There were no accelerometers attached directly to the grids for this test. While the cylindrical ground screen was in place for the integrated assembly vibration tests, the front mask was not installed due to contact with the accelerator grid. The mask contact was not severe, but it would have interfered with screen to accelerator contact measurements during active parts of the test.

A 1/8G sine sweep was applied to the EMT1c, beginning at a frequency of 5 Hz and ending at a frequency of 2000 Hz. Frequency increased at the rate of 2 octaves per minute, and took a total of 256 seconds to complete. Accelerometers on the optics mounting ring indicate a first structural resonance in the thruster at frequency of 104 Hz. See figure 7. The force amplification factor associated with this peak was on the order of 11:1. Coincident with the resonance was evidence of screen to accelerator grid contact as indicated by a brief collapse of the +9 volt bias voltage applied between the two grids. There was a slightly more intense resonance at a frequency of 118 Hz, with an amplification of 12:1. All accelerometer responses above 200 Hz appear fairly chaotic.

### Random Vibration Test

As indicated in the test procedure, plans were to step up random vibration levels over three brief test sessions. The first session was to be at 20% intensity, and the final session was to be at 100% intensity. The level was brought down to zero between sessions so that superficial visual inspection could take place. Specifications for the NSTAR random vibration acceptance levels can be seen in table 2. Occasional screen to accelerator grid contact took place even at low levels of random vibration. At a level of 0.5  $g_{rms}$ , contact occurred randomly about once per second. At a level of 1.2 g, the contact rate increased to about 45 counts per second. While contact was sporadic, an underlying frequency of 109 Hz was easily distinguished using the 9 volt circuit. Random vibration levels beyond 2.5  $g_{rms}$  resulted in almost constant buzzing between the grids at a uniform frequency of 109 Hz. No debris was seen within the thruster during two pauses of the test, so vibration level was finally increased to 9.2  $g_{rms}$  for 60 seconds. Response from an accelerometer located near the ion optics assembly can be seen in figure 8. Contact occurred with a frequency of 108 Hz throughout the

60 seconds at full level. See figure 9. Despite the contact, there was no sign of loose carbon particles breaking free.

The ion optics assembly was removed from the EMT1c, and showed no sign of damage. The only sign of debris was a small amount of carbon dust. The four broken webbing defects that were present in the screen grid prior to testing had not changed. Subsequent high voltage tests were passed with no unusual insulator leakage current. It is quite possible that the carbon dust was originally generated during grid fabrication, and was released as a result of the vibration. The grids were not subjected to any special cleaning procedure upon delivery. It is also possible that the dust was a direct result of vibrational chafing. The volume of dust was very small, and would likely go undetected if it were not concentrated by the debris collector. The screen to accelerator grid contact frequency falls right between the first and second resonances observed during the 1/8 g sine sweep. It is thus likely that the grid contact frequency was driven by the structural dynamics of the thruster rather than the optics alone. Results from the component vibration test showed the dished pyrolytic grids to have a resonant frequency over 2 octaves higher than the contact frequency observed during random vibration.

## CONCLUSIONS

Thirty cm pyrolytic carbon ion thruster optics have been fabricated geometrically similar to the molybdenum ion optics used on NSTAR. They were then installed on EMT3, and experimentally evaluated over much of the original operating envelope. Ion beam currents ranged from 0.51 to 1.76 A, at total voltages up to 1280V. The perveance, electron back-streaming limit, and screen-grid transparency were compared with previous data obtained with molybdenum. While thruster performance with pyrolytic carbon was quite similar to that with molybdenum, behavior variations can reasonably be explained by slight geometric differences. Following all performance measurements, the pyrolytic carbon ion optics assembly was subjected to an abbreviated vibration test. The thruster endured 9.2  $g_{rms}$  of random vibration in the axial direction, similar to DS-1 acceptance levels. Despite significant grid clashing, there was no observable damage to the ion optics assembly.

## REFERENCES

- [1] Haag, T.W., et al, "Carbon-Based Ion Optics Development at NASA GRC," IEPC Paper 01-094, October, 2001.
- [2] AFRL PRDA NR 00-08-MLK, "Topic 9—Reduced Erosion Materials for Electrostatic Thrusters," Spring 2000.
- [3] Mueller, J., Brophy, J.R., and Brown, D.K., "Design, Fabrication, and Testing of 30-cm Dia Dished Carbon-Carbon Ion Engine Grids," AIAA Paper 96-3204, July 1996.
- [4] Meserole, J.S. and Rorabach, M.E., "Fabrication and Testing of 15 cm Carbon-Carbon Grids with Slit Apertures," AIAA Paper 95-2661, July 1995.
- [5] Kitamura, S., et al, "Fabrication of Carbon-Carbon Composite Ion Thruster Grids—Improvement of Structural Strength," IEPC Paper 97-093, October 1997.
- [6] Meserole, J.S., "Measurement of Relative Erosion Rates of Carbon-Carbon and Molybdenum Ion Optics," AIAA Paper 94-3119, June 1994.
- [7] Patterson, M., "High Thrust Density Optics for Advanced Ion Propulsion," Interim Contractor Report: Ceramic Composites Inc. (NASA C-75647-J), February 8, 2001.
- [8] Haag, T.W., and Soulas, G.C., "Performance of 8 cm Pyrolytic-graphite Ion Thruster Optics," AIAA Paper 2002-4335, July 2002.
- [9] Sovey, J.S., et al., "Development of an Ion Thruster and Power Processor for New Millennium's Deep Space 1 Mission," NASA Technical Memorandum 113129, December 1997.
- [10] Rawlin, V.K., et al, "NSTAR Flight Thruster Qualification Testing," AIAA paper 98-3936, July 1998.
- [11] Anderson, J.R., et al., "Results of an On-going Long Duration Ground Test of the DS1 Flight Spare Ion Engine," AIAA Paper 99-2857, June 1999.

| Throttle Level              | TH0  | TH4   | TH10  | TH15  |
|-----------------------------|------|-------|-------|-------|
| Beam Power, kW              | 0.32 | 0.78  | 1.43  | 1.94  |
| Beam P.S. Voltage, V        | 650  | 1100  | 1100  | 1100  |
| Accelerator Voltage, V      | -150 | -150  | -180  | -180  |
| Beam P.S. Current, A        | 0.50 | 0.71  | 1.30  | 1.76  |
| Discharge Flow (Xe, sccm)   | 8.45 | 10.77 | 19.78 | 27.13 |
| Neutralizer flow (Xe, sccm) | 3.6  | 3.6   | 3.6   | 3.6   |

Table 1.—Power set points, and corresponding xenon flow rates into discharge chamber.

| Frequency, Hz           | Vibration Level                     |
|-------------------------|-------------------------------------|
| 20                      | 0.0161 g <sup>2</sup> /Hz           |
| 20 to 50                | +6 dB/Octave                        |
| 50 to 500               | 0.1 g <sup>2</sup> /Hz              |
| 500 to 2,000            | -6 dB/Octave                        |
| 2,000                   | 0.00631 g <sup>2</sup> /Hz          |
| <b>Duration: 60 sec</b> | <b>Overall: 9.2 g<sub>rms</sub></b> |

Table 2.—Random vibration frequency spectrum for NSTAR acceptance levels

|                               | TH0   | TH4   | TH10  | TH15   |
|-------------------------------|-------|-------|-------|--------|
| <b>Accelerator Current</b>    |       |       |       |        |
| Carbon, 100% (mA)             | 1.5   | 2.1   | 6.2   | 10.8   |
| Carbon, 115% (mA)             | 1.9   | 2.3   | 6.9   | 11.5   |
| DS-1 (mA)                     | 2.5   | n/a   | n/a   | 6.8    |
| <b>Elec. Backstream Limit</b> |       |       |       |        |
| Carbon, 100% (Vdc)            | -50   | -91   | -100  | -104   |
| Carbon, 115% (Vdc)            | -45.1 | -84.8 | -92.1 | -94.3  |
| DS-1 (Vdc)                    | -68.3 | n/a   | n/a   | -149.9 |
| <b>Screen Grid Trans.</b>     |       |       |       |        |
| Carbon, 100%                  | .750  | .799  | .765  | .724   |
| Carbon, 115%                  | .728  | .780  | .746  | .694   |
| DS-1                          | .819  | n/a   | n/a   | .819   |

Table 3.—Accelerator impingement current, electron backstreaming, and screen transparency for 30 cm pyrolytic carbon and molybdenum (DSI) optics.<sup>10,11</sup>

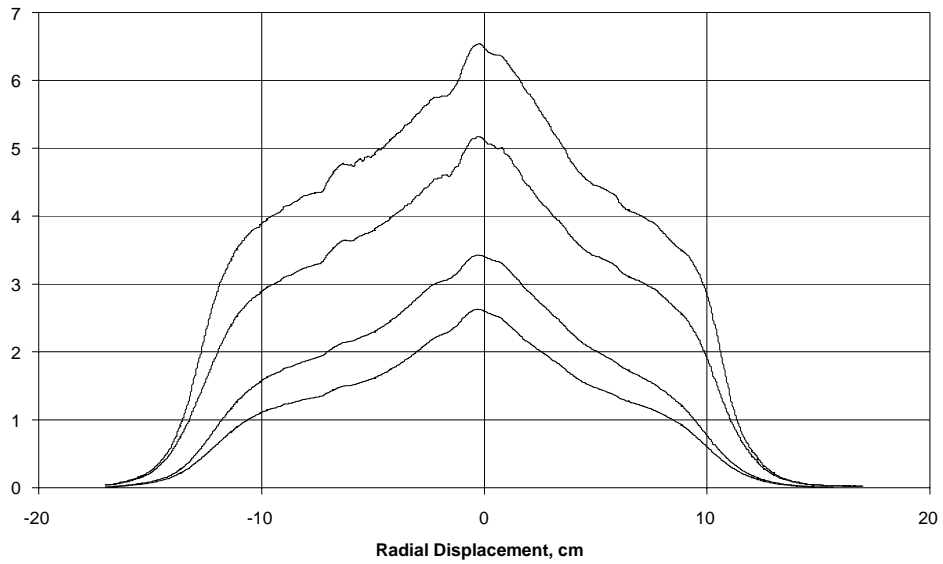


Figure 1.—Plume profile taken with Faraday probe.

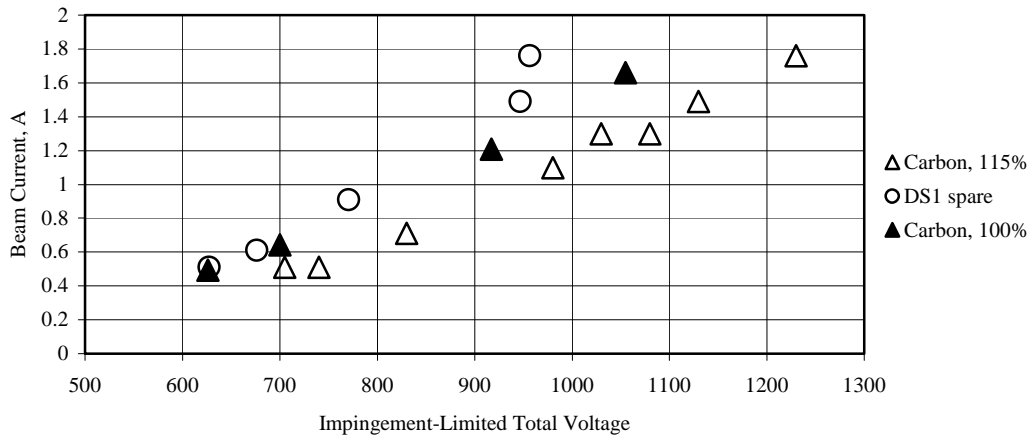


Figure 2.—Perveance of 30 cm carbon and molybdenum ion optics.<sup>10,11</sup>

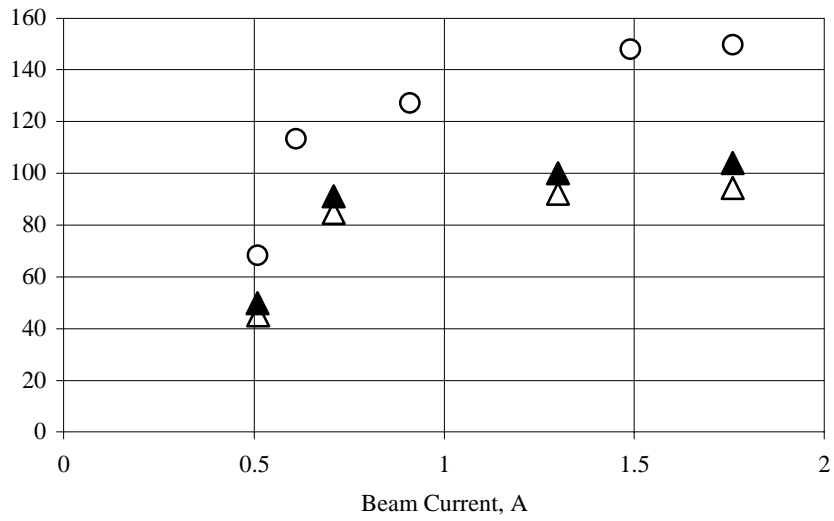


Figure 3.—Electron backstreaming limit as a function of beam current.<sup>10,11</sup>

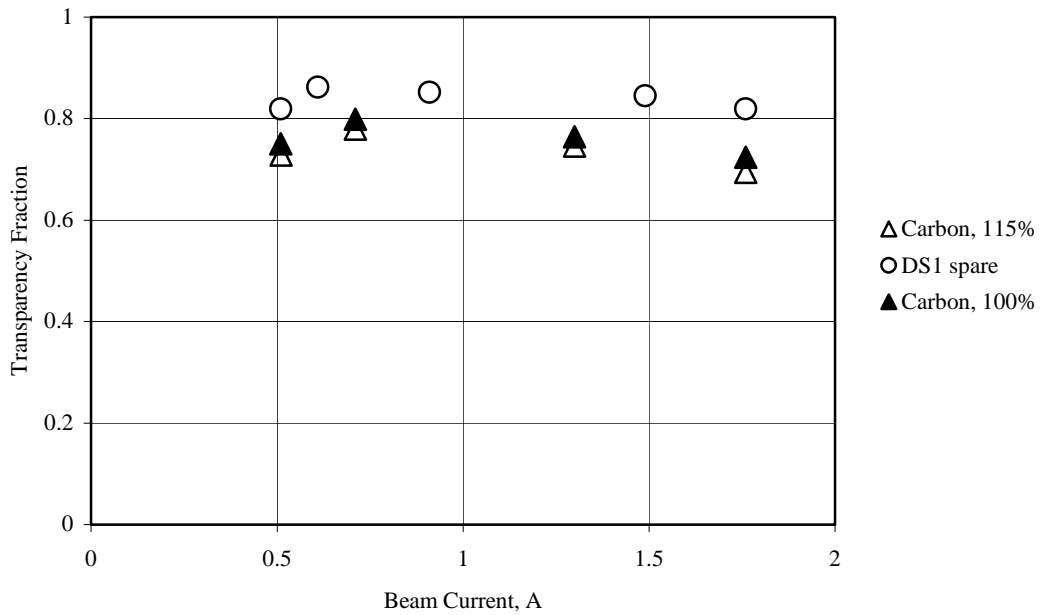


Figure 4.—Screen grid transparency as a function of beam current.<sup>10,11</sup>

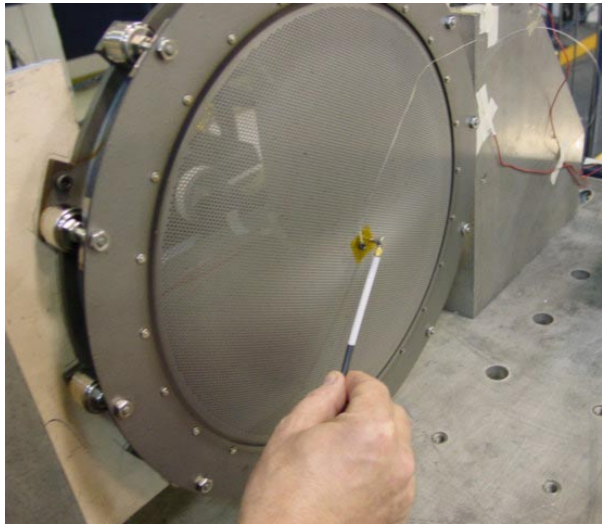


Figure 5.—Thirty cm pyrolytic carbon accelerator grid undergoing component vibration tests.

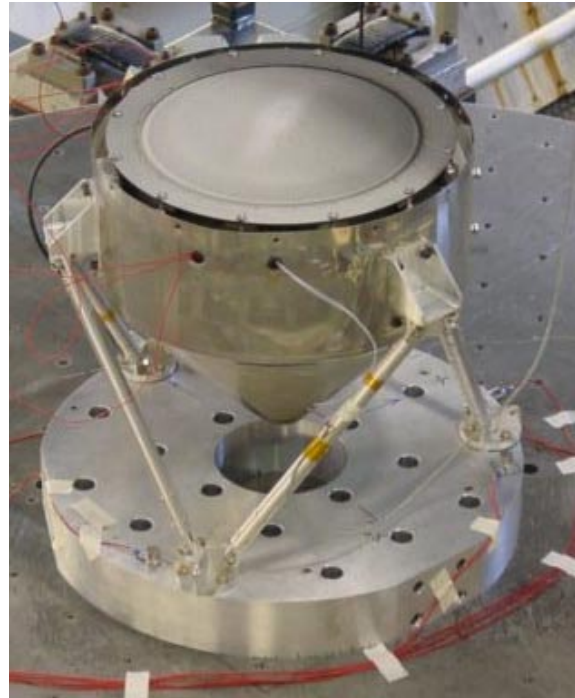


Figure 6.—Thirty cm pyrolytic carbon ion optics installed on EMT1c, undergoing random vibration test.

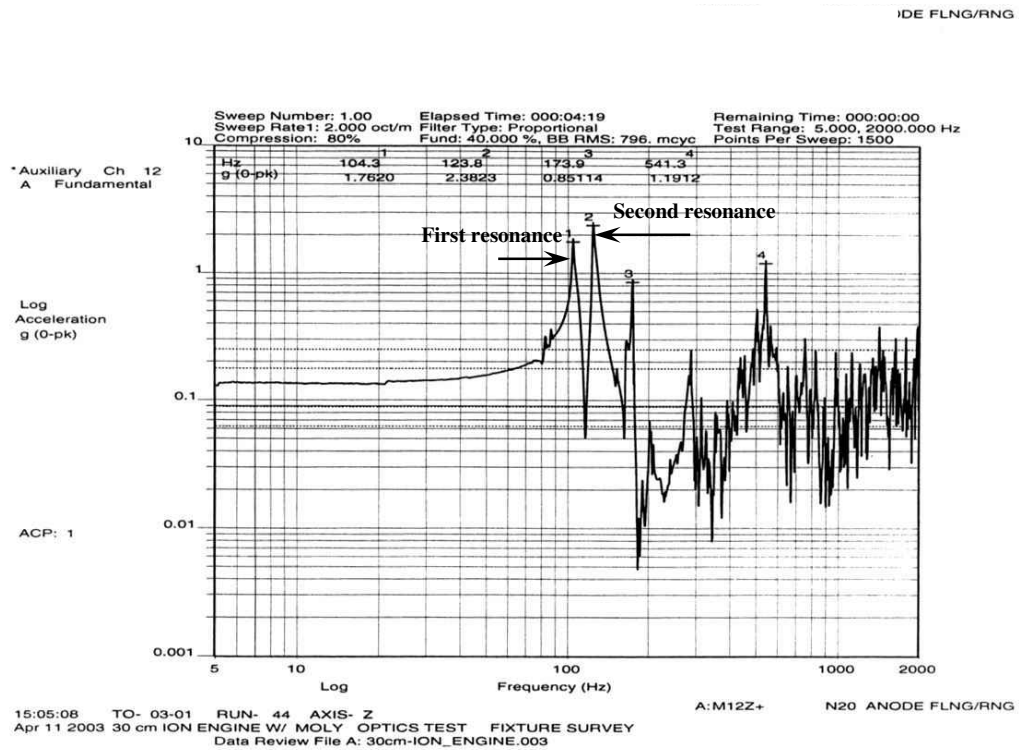


Figure 7.—Accelerometer response near ion optics assembly during 1/8 g sine sweep.

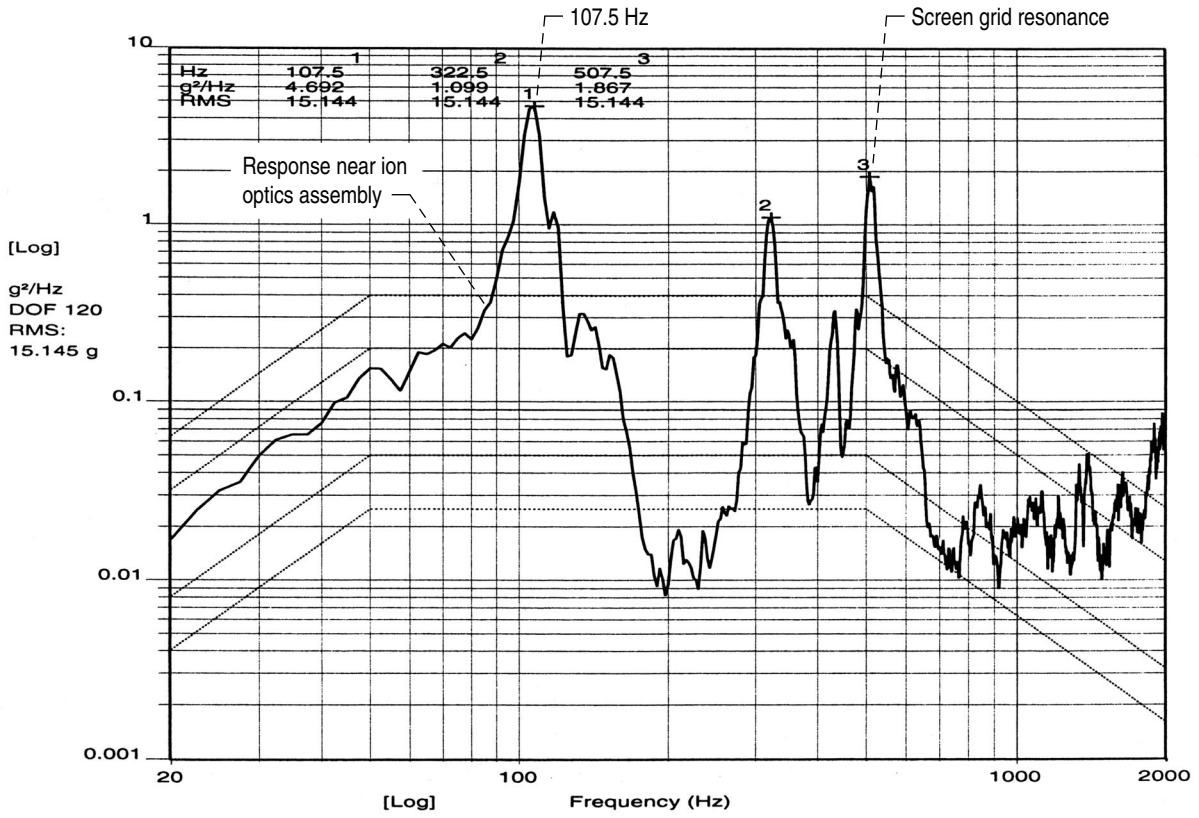


Figure 8.—Frequency spectrum of response accelerometer, 9.2 g.

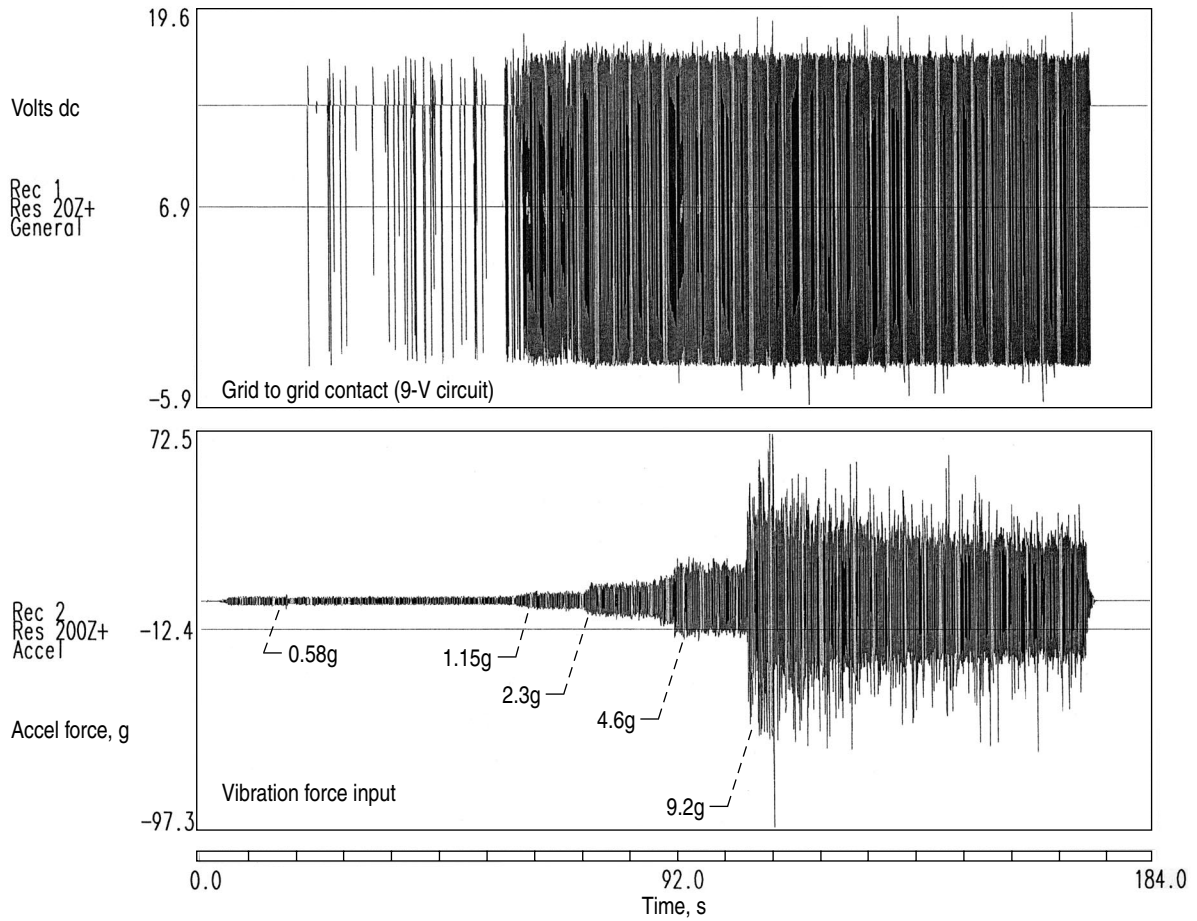


Figure 9(a).—Grid contact as vibration level increases.

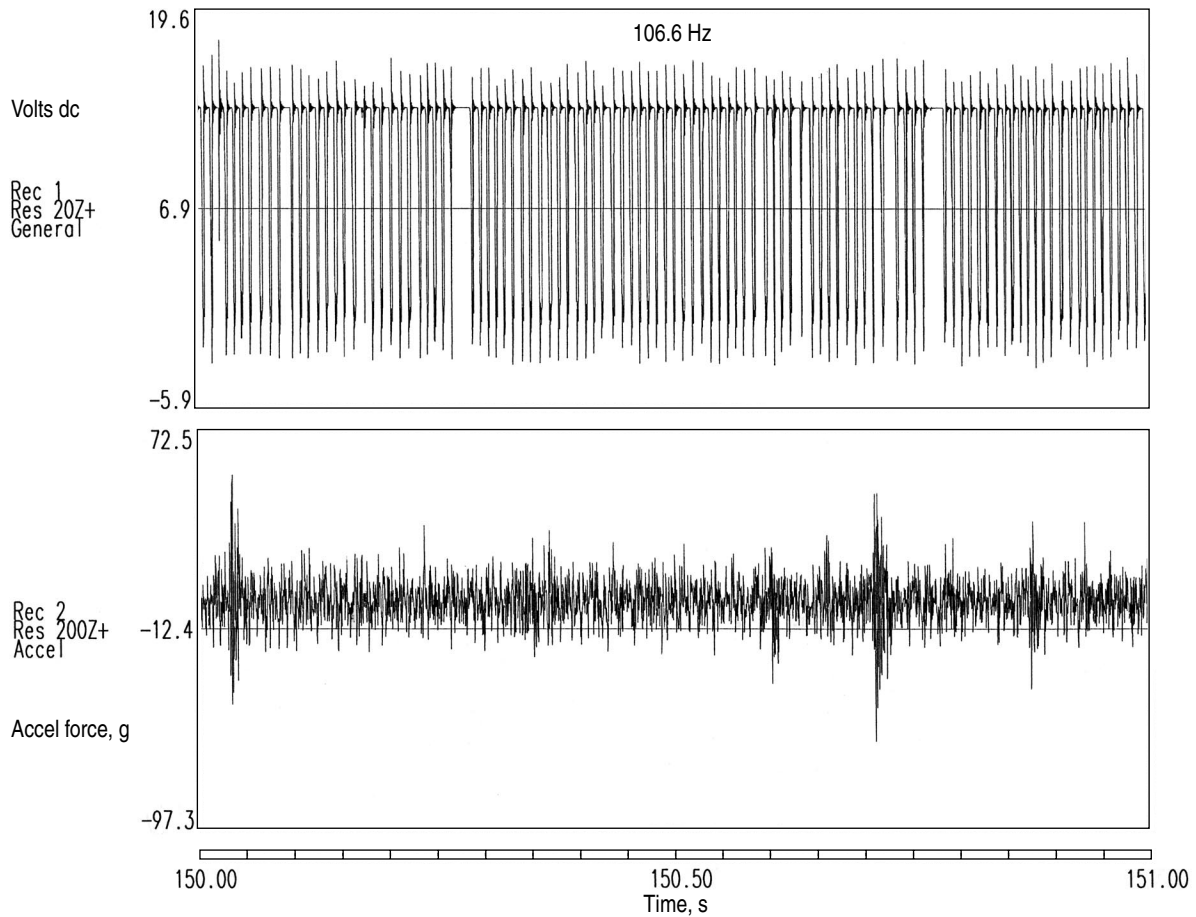


Figure 9(b).—Grid contact at vibration intensity of 9.2 g.

# REPORT DOCUMENTATION PAGE

*Form Approved*  
*OMB No. 0704-0188*

Public reporting burden for this collection of information is estimated to average 1 hour per response, including the time for reviewing instructions, searching existing data sources, gathering and maintaining the data needed, and completing and reviewing the collection of information. Send comments regarding this burden estimate or any other aspect of this collection of information, including suggestions for reducing this burden, to Washington Headquarters Services, Directorate for Information Operations and Reports, 1215 Jefferson Davis Highway, Suite 1204, Arlington, VA 22202-4302, and to the Office of Management and Budget, Paperwork Reduction Project (0704-0188), Washington, DC 20503.

|   |   |  |  |  |
|---|---|--|--|--|
| <b>1. AGENCY USE ONLY</b> ( <i>Leave blank</i> )  |   | <b>2. REPORT DATE</b><br>August 2004                           | <b>3. REPORT TYPE AND DATES COVERED</b><br>Technical Memorandum                                    |  |
| <b>4. TITLE AND SUBTITLE</b><br><br>Performance and Vibration of 30 cm Pyrolytic Ion Thruster Optics  |   |  | <b>5. FUNDING NUMBERS</b><br><br>WBS-22-982-10-02  |  |
| <b>6. AUTHOR(S)</b><br><br>Thomas Haag and George C. Soulas   |   |  |  |  |
| <b>7. PERFORMING ORGANIZATION NAME(S) AND ADDRESS(ES)</b><br><br>National Aeronautics and Space Administration<br>John H. Glenn Research Center at Lewis Field<br>Cleveland, Ohio 44135-3191  |   |  | <b>8. PERFORMING ORGANIZATION REPORT NUMBER</b><br><br>E-14673                                     |  |
| <b>9. SPONSORING/MONITORING AGENCY NAME(S) AND ADDRESS(ES)</b><br><br>National Aeronautics and Space Administration<br>Washington, DC 20546-0001  |   |  | <b>10. SPONSORING/MONITORING AGENCY REPORT NUMBER</b><br><br>NASA TM-2004-213178<br>AIAA-2003-4557 |  |
| <b>11. SUPPLEMENTARY NOTES</b><br><br>Prepared for the 39th Joint Propulsion Conference and Exhibit cosponsored by AIAA, ASME, SAE, and ASEE, Huntsville, Alabama, July 20-23, 2003. Responsible person, Thomas Haag, organization code 5430, 216-977-7423.   |   |  |  |  |
| <b>12a. DISTRIBUTION/AVAILABILITY STATEMENT</b><br><br>Unclassified - Unlimited<br>Subject Category: 20<br><br>Available electronically at <a href="http://gltrs.grc.nasa.gov">http://gltrs.grc.nasa.gov</a><br>This publication is available from the NASA Center for AeroSpace Information, 301-621-0390.   |   |  | <b>12b. DISTRIBUTION CODE</b>  |  |
| <b>13. ABSTRACT</b> ( <i>Maximum 200 words</i> )<br><br>Carbon has a sputter erosion rate about an order of magnitude less than that of molybdenum, over the voltages typically used in ion thruster applications. To explore its design potential, 30 cm pyrolytic carbon ion thruster optics have been fabricated geometrically similar to the molybdenum ion optics used on NSTAR. They were then installed on an NSTAR Engineering Model thruster, and experimentally evaluated over much of the original operating envelope. Ion beam currents ranged from 0.51 to 1.76 A, at total voltages up to 1280 V. The perveance, electron back-streaming limit, and screen-grid transparency were plotted for these operating points, and compared with previous data obtained with molybdenum. While thruster performance with pyrolytic carbon was quite similar to that with molybdenum, behavior variations can reasonably be explained by slight geometric differences. Following all performance measurements, the pyrolytic carbon ion optics assembly was subjected to an abbreviated vibration test. The thruster endured 9.2 g <sub>rms</sub> of random vibration along the thrust axis, similar to DS-1 acceptance levels. Despite significant grid clashing, there was no observable damage to the ion optics assembly. |   |  |  |  |
| <b>14. SUBJECT TERMS</b><br><br>Electric propulsion; Ion thruster   |   |  | <b>15. NUMBER OF PAGES</b><br>19   |  |
|   |   |  | <b>16. PRICE CODE</b>  |  |
| <b>17. SECURITY CLASSIFICATION OF REPORT</b><br>Unclassified  | <b>18. SECURITY CLASSIFICATION OF THIS PAGE</b><br>Unclassified | <b>19. SECURITY CLASSIFICATION OF ABSTRACT</b><br>Unclassified | <b>20. LIMITATION OF ABSTRACT</b>  |  |



